POSTBUCKLING BEHAVIOUR OF ANISOTROPIC PLATES UNDER BIAXIAL COMPRESSION AND SHEAR LOADS

Giulio ROMEO and Giacomo FRULLA
POLITECNICO DI TORINO, Dept. of Aerospace Eng., C.so Duca degli Abruzzi 24, Turin,Italy

Abstract

An analytical solution has been developed to investigate the buckling and postbuckling behaviour of anisotropic plates under biaxial compression and shear loads.The nonlinear differential equations are expressed in terms of the out-of-plane displacement and the Airy stress function and solved, in conjunction with the Galerkin method, in the case of symmetric laminates under various boundary conditions. The results obtained show how boundary conditions and shear load direction affect postbuckling behaviour. A new and original test facility was built in order to apply simultaneously both biaxial compression and shear load. A good correlation between theoretical analysis and experimental results has been obtained.

I. Introduction

Several analytical and experimental works are available regarding buckling of composite panels under combined loads[1-6]; theoretical analysis can predict the buckling load when combined loads are applied. However, in most of cases the experimental results reported are relative to uniaxial compression or shear load only; very few papers report results in which a combination of the two loads was applied. In previous works[7-9] the authors determined the buckling loads of laminated cylindrical shells by solving the Donnel-type linear equations in conjunction with the Galerkin method; both the simply supported and fully clamped boundary conditions were taken into consideration. The ALPATAR computer program was developed for any unsymmetric and unbalanced laminates working out the set of linear algebric equations in the form of an eigenvalue problem.

The experimental results reported in literature show a noticeable postbuckling behaviour of the composite panels before failure. The analytical results reported in literature[2,10-14] generally concern anisotropic panels with various boundary conditions subjected to uniaxial or biaxial loading or simply supported anisotropic panels under biaxial compression and shear loading; experimental results on the buckling and postbuckling behaviour of anisotropic panels under combined load have not been found. On the basis of these considerations, a new test facility was built at the Technical University of Turin in order to apply simultaneously both biaxial compression and shear load.

Furthermore, this paper presents an analytical solution developed to investigate the buckling and postbuckling behaviour of simply supported and/or fully clamped anisotropic plates under biaxial compression and shear loads. The out-of-plane equilibrium and compatibility nonlinear differential equations of an anisotropic plate are expressed in terms of the transverse displacement and the Airy stress function, equations which reduce to the well known ones originally developed by Von Karman in the case of isotropic plate. In the case of an anisotropic and symmetric laminate, the two equations have been solved in conjunction with the Galerkin method. The nonlinear set of equations is converted into a linear sequence by using the modified Powell hybrid method. The POBUCK computer program has been developed to determine the buckling load and the out-of-plane displacement in the postbuckling phase. The results obtained are in a very good agreement with the few analytical results available in literature and in good agreement with the experimental results obtained in our laboratory.

II. Theoretical Analysis

An analytical solution has been developed for the buckling and postbuckling behaviour of anisotropic plates under biaxial compression and shear loads. For many engineering applications the ratio of inplane dimensions to thickness is often greater than 30; in such cases transverse shear deformations are not significant for practical laminates; thus, in a first stage, the shear deformation is not included in the buckling analysis. The plate thickness is denoted by h and the in plane dimensions by a and b; the laminate is symmetric and composed of an arbitrary number of layers with arbitrary fibre orientation in each layer; the midplane

displacements in the x, y and z directions are denoted by u, v and w, respectively.

The Von Karman kinematic relations are assumed for the strain- displacement relations; the Airy stress function is introduced to describe the in-plane loads per unit width:

$$N_x = \psi_{,yy}; \quad N_y = \psi_{,xx}; \quad N_{xy} = -\psi_{,xy} \qquad (1)$$

The following, and other nondimensional parameters are introduced[13]:

$$\xi=x/a; \ \eta=y/b; \ \lambda=a/b; \ U=u/h; \ V=v/h; \ W=w/h;$$

$$F=\psi/(A_{22}h^2); \ [A^]=[A]/A_{22}; [D^]=[D]/(A_{22}h^2)$$

$$\{N^\}=\{N\}(b^2/h^2A_{22}); \ \{M^\}=\{M\}(b^2/h^3A_{22})$$

where A and D are the extensional and bending stiffnesses of the laminate and N and M the force and moment resultant.

By using the principle of the stationary value of the total potential energy, the out-of-plane equilibrium equation associated with the plate compatibility equation give the following set of differential equations, in nondimensional form:

$$D_{11}\hat{}W_{,\xi\xi\xi\xi} + 4D_{16}\hat{}\lambda W_{,\xi\xi\xi\eta} + 2(D_{12}\hat{}+2D_{66}\hat{})\lambda^2 W_{,\xi\xi\eta\eta} + 4D_{26}\hat{}\lambda^3 W_{,\xi\eta\eta\eta} + D_{22}\hat{}\lambda^4 W_{,\eta\eta\eta\eta} = \lambda^2(W_{,\xi\xi}F_{,\eta\eta} + W_{,\eta\eta}F_{,\xi\xi} - 2W_{,\xi\eta}F_{,\xi\eta}) \qquad (2a)$$

$$A_{22}\hat{}^* F_{,\xi\xi\xi\xi} - 2A_{26}\hat{}^*\lambda F_{,\xi\xi\xi\eta} + (2A_{12}\hat{}^* + A_{66}\hat{}^*)\lambda^2 F_{,\xi\xi\eta\eta} - 2A_{16}\hat{}^*\lambda^3 F_{,\xi\eta\eta\eta} + A_{11}\hat{}^*\lambda^4 F_{,\eta\eta\eta\eta} = \lambda^2(W_{,\xi\eta}{}^2 - W_{,\xi\xi}W_{,\eta\eta}) \qquad (2b)$$

where $[A^*] = [A^]^{-1}$. Both the simply supported (BC-1) and fully out-of-plane clamped (BC-3) boundary conditions are taken into consideration; the following conditions should be satisfied:

BC-1)
at $\xi = 0,1$: $W=M_\xi=0$; $F_{,\eta\eta}=n_\xi$; $F_{,\xi\eta}=-\lambda n_{\xi\eta}$.
at $\eta = 0,1$: $W=M_\eta=0$; $F_{,\xi\xi}=\lambda^2 n_\eta$; $F_{,\xi\eta}=-\lambda n_{\xi\eta}$.
(3)

BC-3)
at $\xi = 0,1$: $W=W_{,\xi}=0$; $F_{,\eta\eta}=n_\xi$; $F_{,\xi\eta}=-\lambda n_{\xi\eta}$
at $\eta = 0,1$: $W=W_{,\eta}=0$; $F_{,\xi\xi}=\lambda^2 n_\eta$; $F_{,\xi\eta}=-\lambda n_{\xi\eta}$

The solutions to the governing equations (2) have been assumed to take the following form:

$$F=n_\xi\eta^2/2+n_\eta(\lambda\xi)^2/2-\lambda n_{\xi\eta}\xi\eta+\Sigma\Sigma F_{mn}X_m(\xi)Y_n(\eta)$$

$$W = \Sigma\Sigma C_{mn}\theta_{mn}(\xi,\eta). \qquad (4)$$

where n_ξ , n_η and $n_{\xi\eta}$ are the nondimensional applied external loads and:

$$X_m(\xi)=\cosh\varepsilon_m\xi - \cos\varepsilon_m\xi - \alpha_m(\sinh\varepsilon_m\xi - \sin\varepsilon_m\xi)$$

$$Y_n(\eta)=\cosh\varepsilon_n\eta - \cos\varepsilon_n\eta - \alpha_n(\sinh\varepsilon_n\eta - \sin\varepsilon_n\eta)$$

are the characteristic beam functions corresponding to a beam clamped at each end; the values of the constants ε_m and α_m have been determined with a precision up to 16 digits.

While the Airy stress function remains the same for both the boundary conditions, the following functions were used for the out-of-plane W:

BC-1) $\theta_{mn}=\sin m\pi\xi \sin n\pi\eta$;
BC-3) $\theta_{mn}=X_m(\xi)Y_n(\eta)$ (5)

Likewise, solutions for two other boundary conditions were obtained by considering the opposite ends to be clamped and the sides simply supported (BC-2) and then viceversa (BC-4).

The constitutive equations, with the associated boundary conditions, were solved using the Galerkin method. Second and third- order integrals of the type

$$X^3{}_pX_i d\xi \ ; \quad X^2{}_pX_i d\xi \ ; \quad X^1{}_pX_i d\xi;$$

$$X_mX^2{}_pX_i d\xi; \quad X^2{}_mX_pX_i d\xi; \quad X^1{}_mX^1{}_pX_i d\xi$$

(and many others) appear in the Galerkin coefficients; the apex i denotes a derivative of order i with respect to the ξ-coordinate. These integrals also hold for functions Y_i with η replacing ξ. While the second-order integrals were analytically solved[7], the third- order integrals have been numerically determined using the ABACI "Scientific Desk" Software.

The POBUCK computer program has been developed for working out the set of nonlinear equations in by an iterative scheme. First the system is made linear by eliminating the nonlinear terms; then the buckling load and the corrisponding eigenvector are determined in the form of an eigenvalue problem. This eigenvector is used in the nonlinear system as the starting point of the iteration for determining the postbuckling out-of-plane dispacement at certain loads. The ABACI "Scientific Desk" Software has been used to solve the nonlinear equation based on the modified Powell hybrid method. The software POBUCK operates on IBM PS2, or higher, requiring, with 36 terms, about 5 minutes of CPU by using an NDP Fortran.

The buckling theory developed in the present paper is based, at the moment, on the bifurcation criteria- i.e. that no transverse displacement occurs with increased load until a critical load is reached; however, when an initial imperfection exists, the deflection of the panel increases with the load and converges

with the postbuckling path determined by the bifurcation criteria at values of the load higher than that of buckling. A new theoretical analysis is in progress to include the effects of initial imperfections.

Numerical Results

First a comparison on the postbuckling behaviour of anisotropic panels has been made between the analytical results obtained with the POBUCK computer program and the results found in literature.

Results for square boron/epoxy plates under combined uni and biaxial compression and shear loading[13] are shown in Fig.1; the panel, with $(+45/-45^{\circ})_s$ lay-up, is assumed to be simply-supported along all edges. The material properties used for the computations are: $E_1/E_2=10$; $\nu_{12}=0.3$; $G_{12}/E_2=0.25$. The results correlate very well with those originally obtained by Zhang and Matthews (also for panels with different fiber angles and aspect ratios). In particular, the transverse load and the positive or negative direction of the shear load affect to a great degree the behaviour of anisotropic laminates.

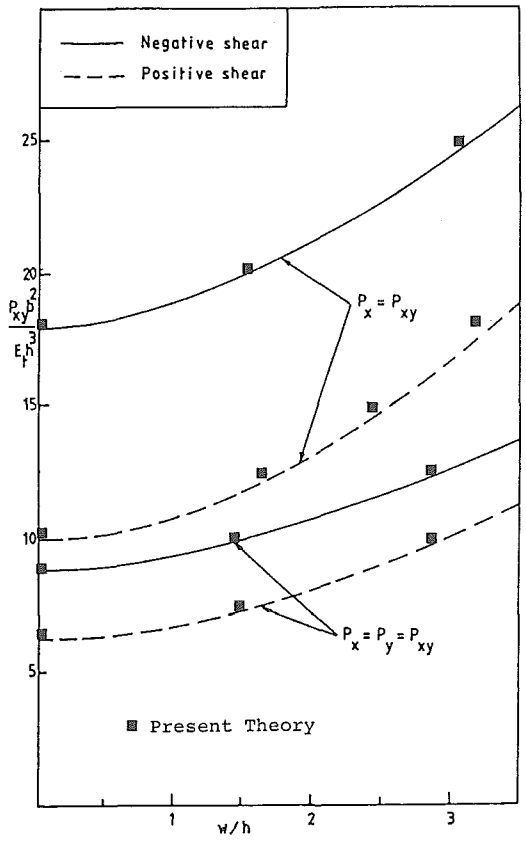

FIGURE 1. Nondimensional central deflection versus nondimensional shear load for square plates with $(\pm 45^{\circ})_s$ lay-up under combined shear and compressive loading (Ref.13).

Results for square graphite/epoxy plates under uniaxial compression[10] are shown in Fig.2; the material properties used for the computations are: $E_1/E_2=40$; $\nu_{12}=0.25$; $G_{12}/E_2=0.5$. The panel, having various fibre orientation, is symmetric and unbalanced and considered to be simply-supported or clamped along all edges. The simply-supported boundary conditions used in the present analysis are different from those used in the reference and then a comparison is not possible. The results correlate very well with those originally obtained by Chia for clamped plates (also under biaxial compression).

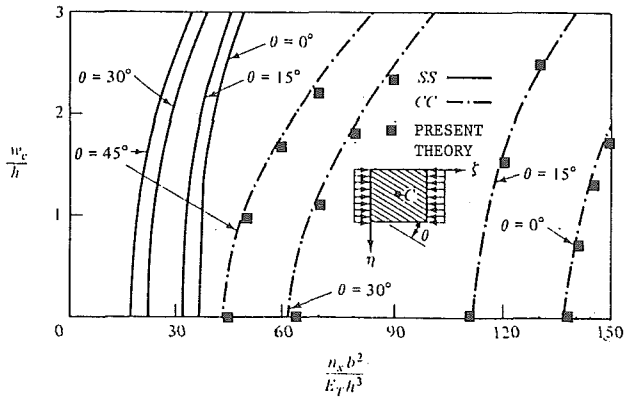

FIGURE 2. Nondimensional central deflection versus nondimensional compression load for square plate with (θ°) lay-up under uniaxial compression (Ref.10).

Results for a square graphite/epoxy orthotropic plate under uniaxial compression[14] are shown in Fig.3; the panel, with $(0/90)_s$ lay-up is considered to be simply supported along all edges. The results correlate very well with those originally obtained in the reference using a finite element analysis as well as with the experimental results there reported.

Finally, results for square boron/epoxy plates under combined uni and biaxial compression and shear loading are shown in Fig.4; the panel, with $(+45/-45^{\circ})_s$ lay-up, is assumed to be clamped along all edges. The Material properties used for the computations are the same of Fig.1. The results of Fig.1 are reported for simply supported plates; however, a comparison is no possible for clamped plates since similar results have not been found in literature. In particular, the results obtained show how boundary conditions, besides transverse load and the positive or negative direction of the shear load, affect to a great degree the behaviour of anisotropic laminates.

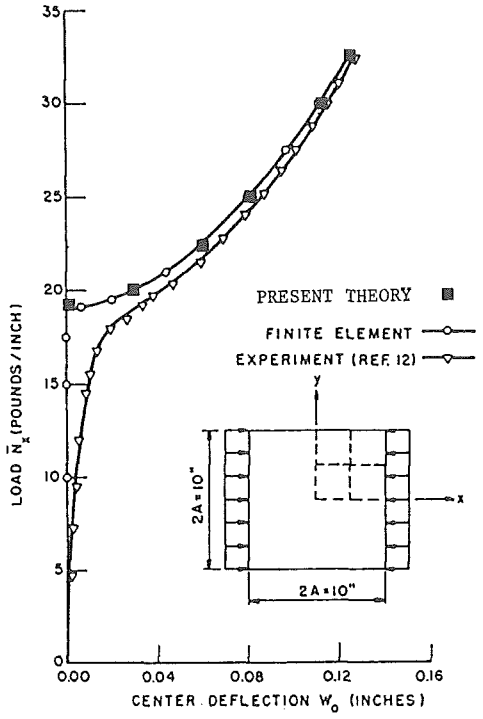

FIGURE 3. Central deflection versus compression load for square plate with $(0/90)_S$ lay-up under uniaxial compression load (Ref.14).

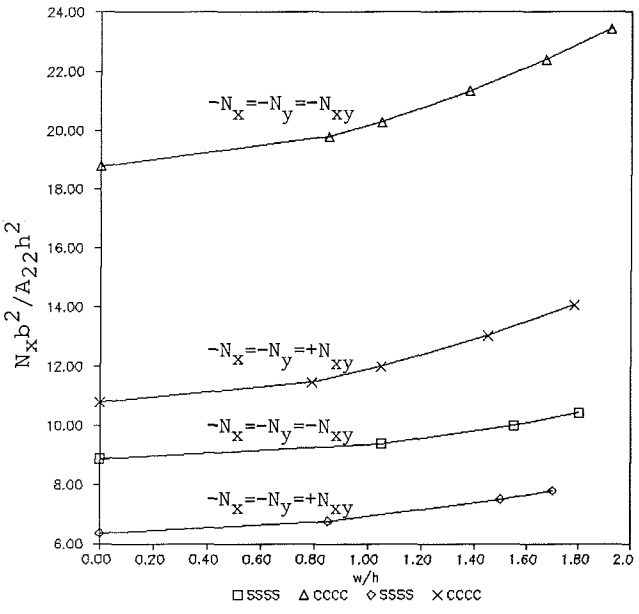

FIGURE 4. Nondimensional central deflection versus nondimensional compression load for simply-supported and clamped square plate with $(\pm 45°)_S$ lay-up under combined biaxial compression and shear loading.

III. Postbuckling Results for Panel Under Combined Biaxial Compression and Shear Loads

Several experimental tests have been carried out by the authors in the past on flat composite panels under uniaxial compression or shear load only; the panels had several boundary conditions, lay-up and shear load directions (positive and negative)[8]. However, in actual conditions, aerospace panels are subjected primarily to biaxial compression and shear load. Since experimental results in this regard were not found in literature, a new testing machine has been built by the Italian company AIP Studio in order to apply simultaneously both biaxial compression and shear load (Fig.5). A maximum longitudinal compression load of 490 kN, a transverse compression or tension load of 196 kN and a positive or negative shear load of 196 kN can be applied to panels with dimensions lower than 1000 by 700 mm. The facility has been predisposed to apply (in the future) tension loads in the longitudinal direction also, as well as fatigue loads (in this case at half values of the above loads).

The load and supporting frames are made of steel alloy and 2024 aluminium alloy. Longitudinal load is applied by two separately controlled servo-actuators; a displacement control is used to maintain the panel ends parallel to each other, their angular rotation controlled to zero with an accuracy of 0.001 degrees. Transverse load is applied by two separately controlled servo-actuators to mantain the panel sides parallel to each other; the transverse load application system floats in order not to interfere with the longitudinal and shear loads. Shear load is applied to the bottom end of the panel by one servo-actuator . The test rig is completely loop controlled via electronic modules closed by 9 transducers. The test rig can apply different load configurations than those reported above, since the actuators can apply both tension and compression loads independently of each other. The frame test fixture used for applying loads to the panel is composed of two L steel rails bolted to the four edges of the specimen and to the flat ends of the testing machine; the panel was assumed to be clamped along all edges.

Several experimental tests were first carried out on a flat panel to verify the buckling load correlation between the analytical results obtained using the ALPATAR code[7], and experimental results[9]. These experimental results are reported in this paper and compared with the analytical results obtained with the present the-

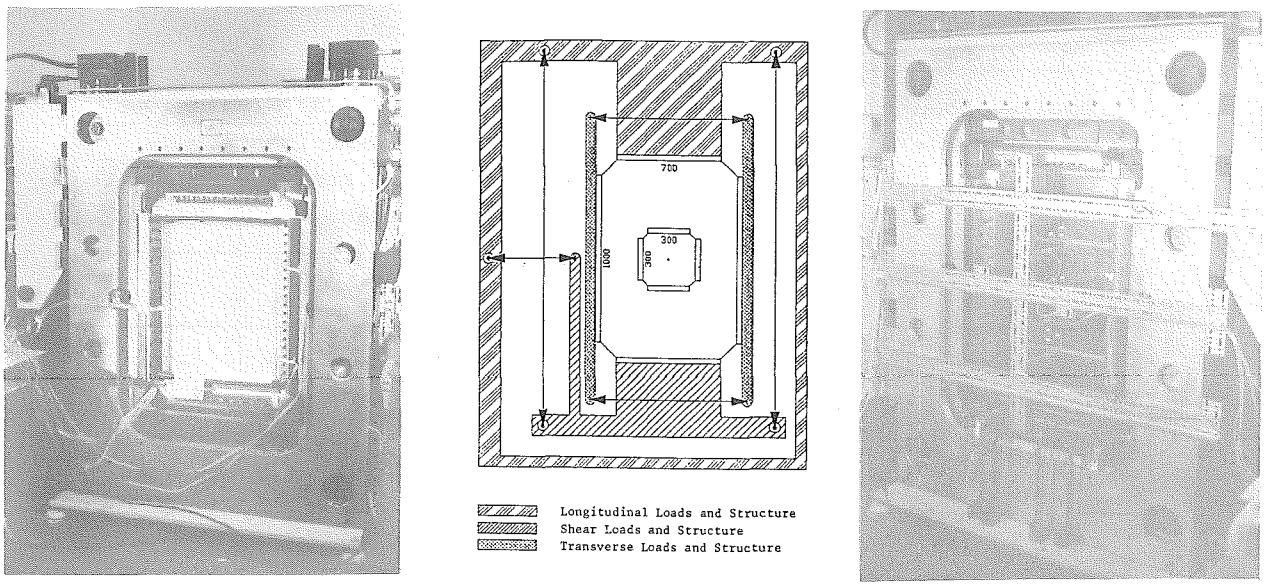

FIGURE 5. The new testing machine to apply simultaneously longitudinal compression, transverse compression or tension and positive or negative shear loading.

ory by using the POBUCK code. Several experimental tests were then carried out on a second flat panel to analyze the postbuckling behaviour and the correlation between the analytical results obtained using the POBUCK code and the experimental results.

The panels were manufactured by using graphite epoxy material, vacuum bagged and autoclave cured. Geometrical data are reported in Table 1 and Table 2 for panels N.1 and N.2, respectively.

49 strain gauges, either linear or rosette, were back to back bonded to several points of the the panel in order to measure in plane strains. Out-of-plane displacements were monitored using the shadow moirè method, and fringe patterns were recorded by a camera to obtain a qualitative behaviour. Furthermore, 9 inductive transducers were placed in contact with the panels at different points in order to measure the displacement values.

Lay-up: $(+45_2/0_4/-45_2/90_2)_{3s}$; thickness=7.74 mm; a=880 mm; b=580 mm.
E_1=218.3 GPa; E_2=6.97 GPa; G_{12}=4.0 GPa; ν_{12}=.305

Applied Load Ratio			Buckling Load per unit width [N/mm]						
			Analytical Present theory			Experimental			
						Membrane strain constant			Southwell Method
N_x/N_x	N_y/N_x	N_{xy}/N_x	N_x	N_y	N_{xy}	N_x	N_y	N_{xy}	N_x
-1	0	0	-857	0	0	-846	0	0	-936
-1	-.2	0	-708	-142	0	-775	-155	0	-798
-1	-.2	+.5	-575	-115	287	-550	-110	275	-578
-1	-.4	0	-552	-221	0	-560	-224	0	-612
-1	-.4	+.5	-475	-190	238	-450	-182	228	-478

TABLE 1: ANALYTICAL AND EXPERIMENTAL RESULTS FOR CLAMPED PANEL N.1 UNDER COMBINED BIAXIAL COMPRESSION AND SHEAR LOAD.

Lay up: $(-45/0_4/+45/90)_{3s}$; thickness=5.52 mm; a=877 mm; b=577 mm.
E_1=209.3 GPa; E_2=6.89 GPa; G_{12}=4.26 GPa; ν_{12}=.305

Applied Load Ratio			Buckling Load per unit width [N/mm]						
			Analytical Present theory			Experimental			
						Membrane strain constant			Southwell Method
N_x/N_x	N_y/N_x	N_{xy}/N_x	N_x	N_y	N_{xy}	N_x	N_y	N_{xy}	N_x
-1	0	0	-297	0	0	-285	0	0	-305
-1	-.4	0	-166	-66	0	-153	-61	0	-164
-1	-.4	+.5	-160	-64	+80	-145	-58	+73	-153
-1	-.4	-.5	-143	-57	-71	-125	-50	-63	-148

TABLE 2: ANALYTICAL AND EXPERIMENTAL RESULTS FOR CLAMPED PANEL N.2 UNDER COMBINED BIAXIAL COMPRESSION AND SHEAR LOAD.

Several tests were carried out on the panels: uniaxial compression, biaxial compression, biaxial compression and shear load. Shear load was applied to the first panel only in the positive direction. A summary of the results are reported in Tables 1 and 2, together with the theoretical buckling load obtained through the analysis reported in paragraph II. The loads per unit width are reported. The critical load at which the panel displayed buckling was defined by load versus strain curves as the value at which the membrane strain does not increase further. For thick panels like those tested, it is more appropriate to use membrane strain instead of the value at which surface strain reversal occurs. Results are also reported for the buckling loads obtained from experimental load deflection via the Southwell method.

Experimental results obtained for the panel N.1 under biaxial compression and shear are reported in Fig.6; transverse and shear loads are, respectively, 40% and 50% of the longitudinal load. The applied load is reported as a function of two back to back strain gauges placed at mid length and mid width). The membrane strain is also reported. Buckling occurred in one main half wave at a longitudinal load of 261 kN (450 N/mm), 5% lower the theoretical value obtained with the POBUCK code. At this value, there was no further increase in membrane strain at half width, both at half length and quarter length from the bottom and top edges.However, strain gauges placed near to the sides still registered an increase in the membrane value; surface strains generally showed a reversal at a lower load. The out-of-plane displacement, as monitored by the shadow moirè, is reported in the same figure and the effective longitudinal load in kN is also shown. A 47% reduction in the longitudinal buckling load was obtained, as an effect of the combined loads, with respect to the uniaxial compression test. More details on the results of this panel are reported in (12).

An initial imperfection was measured on the second panel with a maximum deflection of 1.18 mm in the centre. Experimental results obtained for this panel under biaxial compression are reported in Fig.7; transverse load is 40% of the longitudinal load. Owing to the presence of an initial imperfection, strains measured by back-to-back gauges were not uniform with the load from the start. Buckling occurred in one half wave at a load of 88 kN (153 N/mm), 8,5% lower the theoretical value obtained with the POBUCK code. At this value, there was no further increase in membrane strain at half width, at half length and quarter length from the bottom and top edges. However, strain gauges placed near to the sides still registered an increase in the membrane value. Using the Southwell method, the experimental buckling load coincide with the theoretical value. The out-of-plane displacement recorded in the centre of the panel is reported as a function of the applied longitudinal load; both the experimental results and the analytical results obtained (with 16 terms) through the present analysis can be seen. As expected, the presence of an initial imperfection meant that the experimental transverse displacement increased with the load from the start. Indeed the theoretical results, based on the bifurcation criteria assume zero deflection up to the

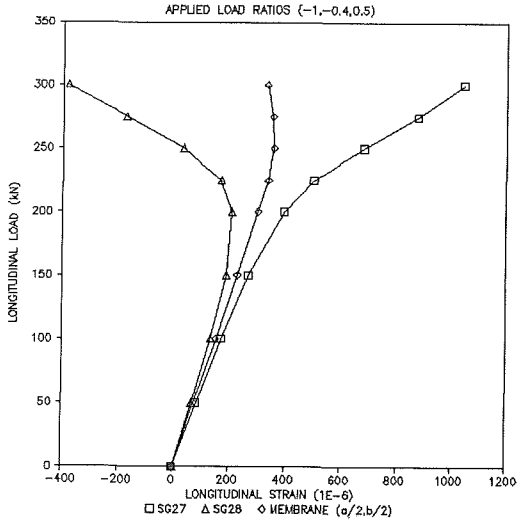

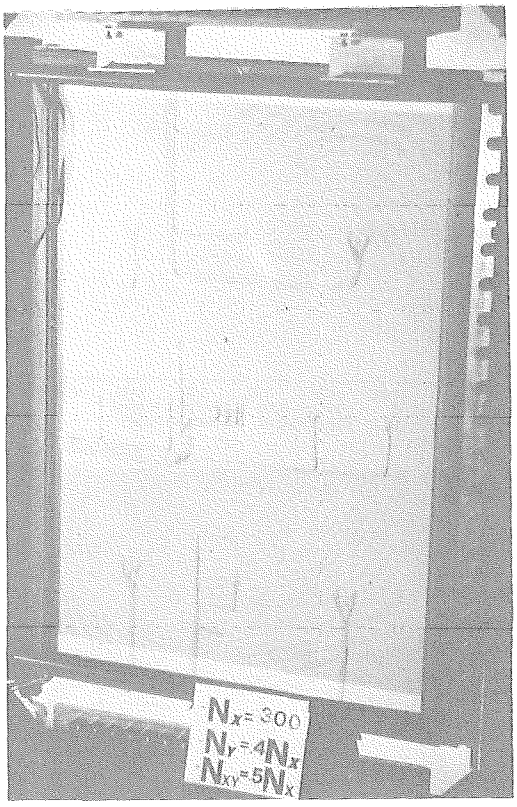

FIGURE 6. Experimental load-strain curves and shadow-moiré patterns of the clamped panel N.1 under biaxial compression and shear loading (N_y=40% N_x; +N_{xy}=50% N_x)

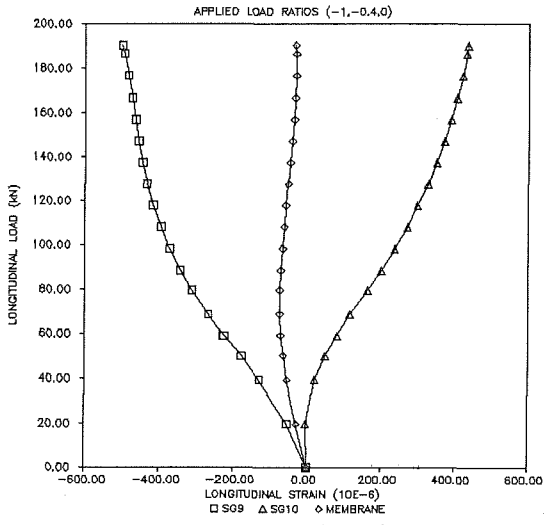

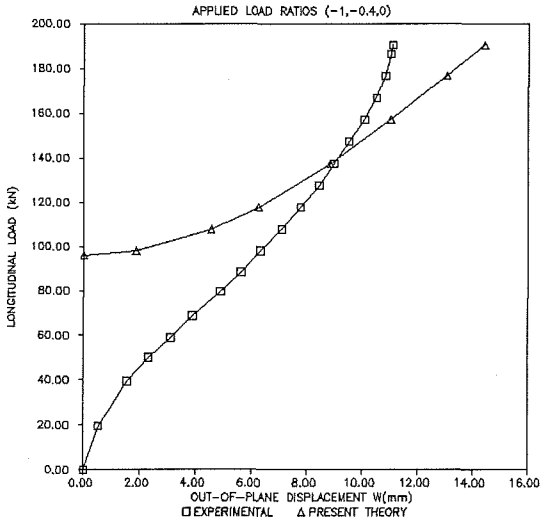

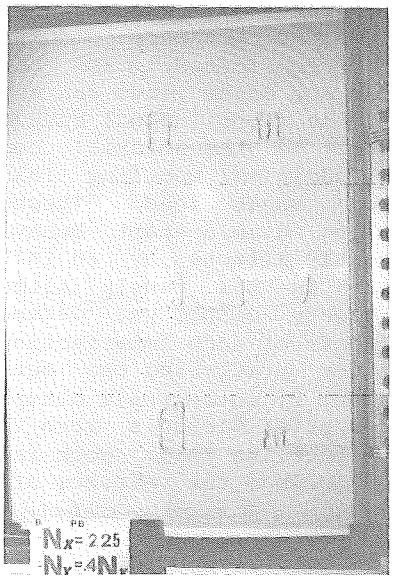

FIGURE 7. Experimental load-strain curves (above) and analytical and experimental central deflection (centre) of the clamped panel N.2 under biaxial compression loading (N_y=40% N_x)

buckling load. However, in the postbuckling phase, the analytically determined out-of-plane displacement are not converging with the experimental path; at a load 40% higher than buckling, the experimental transverse displacement curve intersects the analytical one and diverges from it. This intersection seems due to the initial imperfection and to the anisotropy of the panel with respect to the classical behaviour of isotropic one.

Experimental results obtained for the panel under biaxial compression and positive or negative shear load are reported in Fig.8 and 9, respectively; the transverse and shear loads are, respectively, 40% and 50% of the longitudinal load. The same behaviour of the former tests has been recorded. As it is very clear from these results, the effect of the shear load, as difference with the previous test, is not so high as reported in Fig.1 and this is mainly due to the panel lay-up.

IV. CONCLUSION

With the new testing machine manufactured for the simultaneous application of combined loads, it has been possible to verify for the first time the correlation between theoretical analysis and experimental results on the buckling and postbuckling behaviour of fully clamped composite panels under combined biaxial compression and shear loads.

Test results for composite panels under combined loads correlate well with theoretical results when anisotropic stiffnesses and boundary conditions are adequately considered. In particular, transverse and shear loads can affect considerably the longitudinal buckling load with respect to the uniaxial compression load. In addition, buckling load is affected by shear load direction and postbuckling displacement behaviour is significantly affected by an initial imperfection in the panel. Although the present theory cannot yet determine the exact effects of such imperfections, it is adequate for predicting the out-of-plane displacement of anisotropic clamped panels when the applied load is more than 100% above the buckling load. Work is in progress to include the effects of initial imperfections and load eccentricity.

V. References

1.Starnes J.H.,Dickson J.N.,Rouse M. "Postbuckling behaviour of graphite epoxy panels" in ACEE Composite Structures Technology NASA CP 2321 (1984) pp 137-159.

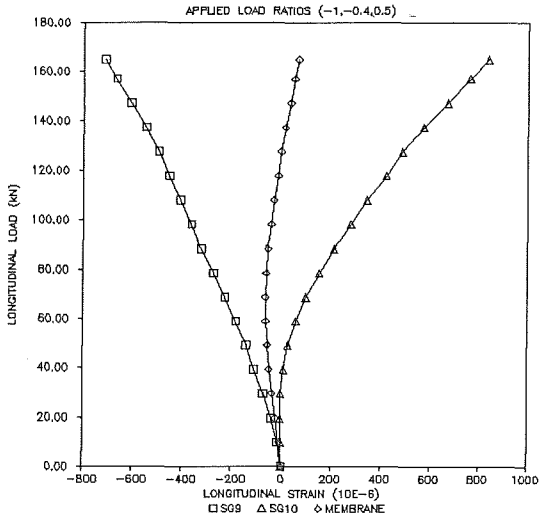

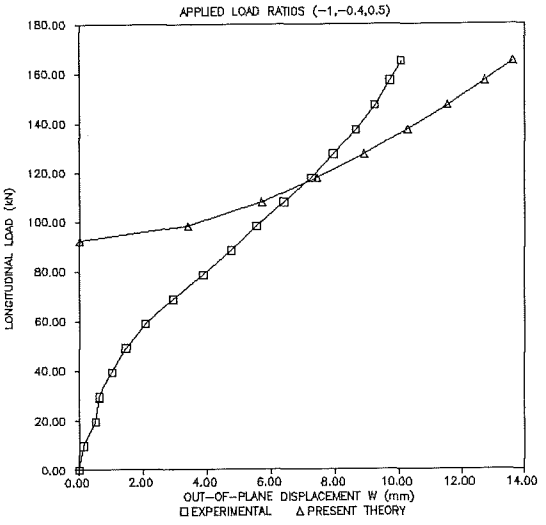

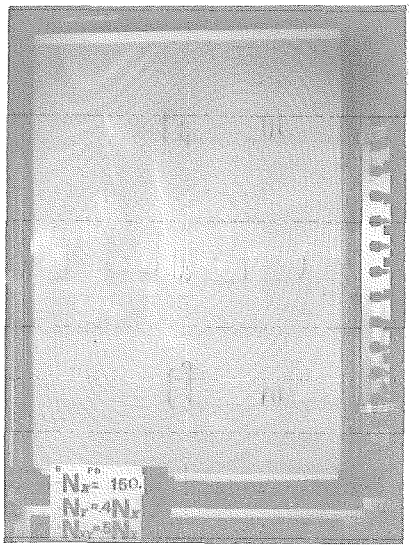

FIGURE 8. Experimental load-strain curves (above) and analytical and experimental central deflection (centre) of the clamped panel N.2 under biaxial compression and positive shear loading (N_y=40% N_x; $+N_{xy}$=50% N_x).

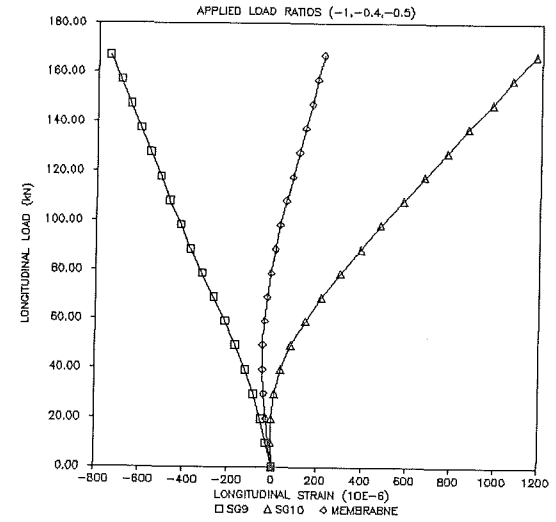

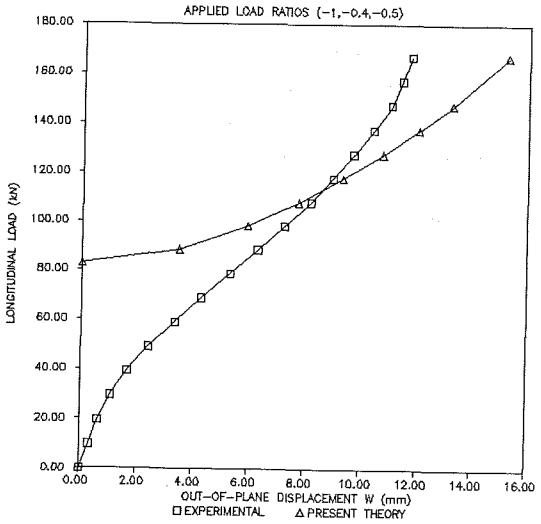

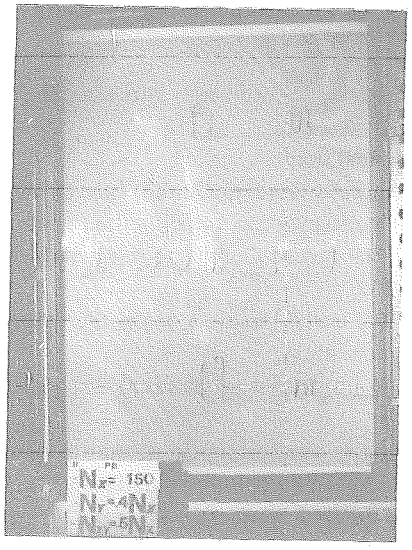

FIGURE 9. Experimental load-strain curves (above) and analytical and experimental central deflection (centre) of the clamped panel N.2 under biaxial compression and negative shear loading (N_y = 40% N_x; $-N_{xy}$ = 50% N_x).

2.Leissa A.W. "Buckling of laminated composite plates and shell panels" AFWAL TR-85-3069 (1985).

3.Whitney J.M. "Buckling of anisotropic laminated cylindrical plates" AIAA J. 22 (1984) pp 1641-1645.

4.Lagace P.A. "Buckling of unsymmetric composite laminates" Composite Structures 5 (1986), pp 101-123

5.Sheinman I. "Bifurcation buckling analysis of stiffened laminated composite panels" in Buckling of Structures (Elsevier, ed.) (1988) pp 355-380.

6.Jun S. & Hong C. "Buckling behaviour of laminated composite cylindrical panels under axial compression" Computer & Structures 29 (1988), pp479-490.

7.Romeo G.,Alonso C.,Pennavaria A. "Buckling of laminated cylindrical plates including effects of shear deformation" in Space Application of Advanced Structural Materials ESA SP-303 (1990) pp. 365-370.

8.Romeo G. & Frulla G. "Buckling of simply supported and clamped anisotropic plates under combined loads" in Spacecraft Structures and Mechanical Testing ESA SP-321 (1991) pp 161-166

9.Romeo G. & Frulla G. "Buckling behaviour of simply supported and clamped anisotropic plates under combined loads" VIII ICCM (1991)

10.Chia C.Y. "Nonlinear Analysis of Plates" (McGraw-Hill ed.) (1980)

11.Prabhakara M.K. "Post-buckling behaviour of simply-supported cross ply rectangular plates" Aeronautical Quarterly (1976) pp 309-316.

12.Sheinman I. & Frostig Y. "Nonlinear analysis of stiffened laminated panels with various boundary conditions" J. Composite Materials, 25 (1991) pp 634-649.

13.Zhang Y. & Matthews F.L. "Postbuckling behaviour of anisotropic laminated plates under pure shear and shear combined with compressive loading" AIAA J. 22 (1984) pp 281-286.

14.Schmit L.A. & Monforton G.R. "Finite deflection discrete element analysis of sandwich plates and cylindrical shells with laminated faces" AIAA J. 8,8 (1970) pp 1454-1461.

Acknowledgments

The research has been carried out by the financial sponsorship of the Ministry of University. Authors would like to acknowledge the efficacious cooperation of G. Ruvinetti and of L. Buco, last year undergraduate in aeronautical engineering.